

Constrained Online Recursive Source Separation Framework for Real-time Electrophysiological Signal Processing

Yao Li, Haowen Zhao, Yunfei Liu, Xu Zhang*

Abstract — Processing electrophysiological signals often requires blind source separation (BSS) due to the nature of mixing source signals. However, its complex computational demands make real-time applicability challenging. This paper presents a novel BSS framework termed constrained online recursive source separation (CORSS) for online processing electrophysiological signals. In the framework, a stepwise recursive unmixing matrix learning rule was adopted to enable real-time updates with minimal computational cost. By incorporating prior information of target signals to optimize the cost function, the framework algorithm converges more readily to actual sources, yielding precise separated sources. The proposed framework was customized and applied to two downstream tasks, real-time surface electromyogram (sEMG) decomposition and real-time respiratory intent monitoring based on diaphragmatic electromyogram (sEMGdi) extraction. The results demonstrated superior performance compared to alternative methods, achieving a matching rate of $96.00 \pm 2.04\%$ for the sEMG decomposition task and $98.12 \pm 1.21\%$ for the sEMGdi extraction task. Our method also exhibits minimal time delay during computation, reflecting its streamlined updating rule as well as excellent real-time capabilities, with only 12.5ms delay when the block size is 0.1s, demonstrates strong performance for real-time processing. Our work shows great significance for applications in real-time human-computer interaction and clinical monitoring.

Index Terms—Online blind source separation, Recursive independent component analysis, Constrained independent component analysis.

I. INTRODUCTION

Electrophysiological signal generated by neuronal discharge reflecting the neural events of human activity [1]. By processing electrophysiological signals collected from different anatomical sites, we can non-invasively extract precise neural commands from the central nervous system for various human-machine interaction tasks [2]. Considering that many tasks require high real-time responsiveness in many fields, there are substantial demands for robust online electrophysiological signal processing.

Unlike existing applications that extract simple features from signals in real-time [3], more sophisticated downstream

tasks such as signal decomposition and electrophysiological signal denoising necessitate blind source separation (BSS) techniques like independent component analysis (ICA) [4]. The signal model of ICA assumes the multi-channel signal under processing as a mixture of weakly dependent latent non-Gaussian sources [5]. While prior work has used ICA and its variants to achieve significant advancements in sEMG signal processing, most approaches involve large-scale data processing and are only suited for offline applications [6]. For instance, commonly used algorithms such as Infomax ICA and FastICA are computationally intensive and unsuitable for scenarios requiring real-time BSS tasks [7].

Several researchers have explored methods for performing online blind source separation. Zhao et al. [6, 8, 9] introduced a series of online BSS methods specifically designed for precise surface signal decomposition. Their approach involves offline computation and adaptive updating of the unmixing matrix (also known as demixing matrix or separation matrix) for online use, thereby achieving stable online performance. While this dual-threaded method has demonstrated good accuracy, its computational demands during offline steps are comparable to conventional ICA methods, indicating no fundamental change in unmixing matrix learning rules.

Other researchers have employed learning rule adaptations to enable real-time usability of ICA algorithms by dynamically updating the unmixing matrix. Two primary learning rules are based on least mean squares (LMS) and recursive least squares (RLS) [10]. These algorithms can be used to deal with spatiotemporal nonstationary data commonly encountered in real-world applications [11, 12]. However, LMS-type algorithms, employing stochastic gradient descent, are computationally straightforward but require careful selection of learning rates for stable convergence [13]. In contrast, RLS-type algorithms accumulate past data exponentially with Sherman-Morrison matrix inversion for faster convergence and improved tracking capabilities, albeit at the cost of increased computational complexity [14, 15]. AKHTAR et al. [16] proposed an Online Recursive ICA (ORICA) based on an RLS-type recursive rule, which achieves fast convergence and low computational complexity by solving a fixed-point approximation. Despite its utility in processing various signal types, like other ICA methods, ORICA only perform well in extracting signals of interest in “simplistic” cases [17]. When facing the complex mixture of unknown source signals typically found in real-world surface electrophysiological recordings, it often suffers from incomplete separation among source signals due to the lack of prior knowledge about the

This work was supported in part by the Anhui Provincial Key Research and Development Project under Grant 2022k07020002. (*Corresponding authors: Xu Zhang.*)

Y. Li, H. Zhao, Y. Liu, X. Zhang are with the School of Microelectronics at University of Science and Technology of China, Hefei, Anhui, China. (xuzhang90@ustc.edu.cn).

target-relevant signals, thereby leading to degraded performance.

Some researchers find that incorporating more assumptions and prior information can avoid local minima and increases the quality of the separation [18]. Stone et al. proposed in [19] that optimal signal separation using Infomax ICA occurs when the contrast function closely matches the cumulative distribution function (CDF) of the target source to be extracted. Building upon this principle, a constrained ICA (cICA) approach was designed for real-time cardiac artifact rejection in [20], utilizing a cICA method that aligns with the probability CDF of electrocardiogram (ECG) signals for artifact removal. Nonetheless, the authors noted that the computation of the unmixing matrix in this method remains overly complex, indicating a need for faster estimation methods.

Given the challenges highlighted in the previous works, this study presents a novel constrained online recursive source separation (CORSS) framework for real-time electrophysiological signal processing. With the recursive learning rule as well as prior knowledge of the target signal to optimize the cost function, the proposed framework facilitates the real-time extraction of precise source signals from surface electrophysiological recordings. This framework was validated through two tasks: real-time sEMG decomposition and real-time extraction of surface diaphragmatic electromyogram (sEMGdi) signals, utilizing collected experiment data. The proposed framework represents a pioneering method in real-time electrophysiological signal processing, offering significant implications for real-time myoelectric control, clinical intelligent monitoring, as well as provide valuable insights into human-machine interaction.

II. RELATED WORKS

A. Blind Source Separation

In BSS tasks, the objective is to separate or recover a set of mixed sources from a set of measured mixtures, which can be expressed as:

$$x(n) = As(n) + v(n) \quad (1)$$

where $x(n) = [x_1(n), x_2(n), \dots, x_M(n)]^T$ is the mixture signal vector with the observed mixture $x_i(n), i = 1, 2, \dots, M$, $s(n) = [s_1(n), s_2(n), \dots, s_N(n)]^T$ is the source signal vector with

$s_i(n), i = 1, 2, \dots, N$ be the scalar source signal vector for a mixing matrix A , $v(n) = [v_1(n), v_2(n), \dots, v_M(n)]^T$ is the vector for uncorrelated additive-random noise, and n is the discrete-time index. The goal is to process $x(n)$ by an adjustable unmixing matrix $W(n)$ such that

$$y(n) = W(n)x(n) \quad (2)$$

contains estimated signals $y(n)$ (also known as component matrix) from source signals $s(n)$. Since the original BSS algorithm such as ICA are typically run in a batch mode [21] in order to keep stochasticity of the empirical gradient low, they are not quite suitable for online implementation in real-time settings.

B. Online progressive FastICA peel-off (PFP)

Chen et al. [22] addressed the issue of FastICA's inability to separate weak source signals in the field of sEMG decomposition by developing an offline progressive FastICA peel-off (PFP) framework. It used constrained FastICA that combines the prior information to access more accurate source signals. Based on this, Zhao et al. [9] introduced an adaptive online PFP method, employing dual-thread operation. They perform offline constrained FastICA to get unmixing matrix updates for online execution, enabling real-time decomposition. This method demonstrates that using constrained FastICA combined with prior information can yield more accurate results. However, this dual-thread approach with offline constrained FastICA inherently leads to increased computational load and latency.

C. Real-time cICA

Breuer et al. [20] proposed a method based on cICA that enables real-time artifact rejection. They initially utilized the demixing matrix from the preceding data segment as the optimal initial matrix, therefore suitable for real-time calculation. Moreover, they used a block-update rule (also known as block update rule) to update the unmixing matrix of the algorithm based on the prior information for ECG extraction, as described in formula (3) of the Infomax ICA algorithm:

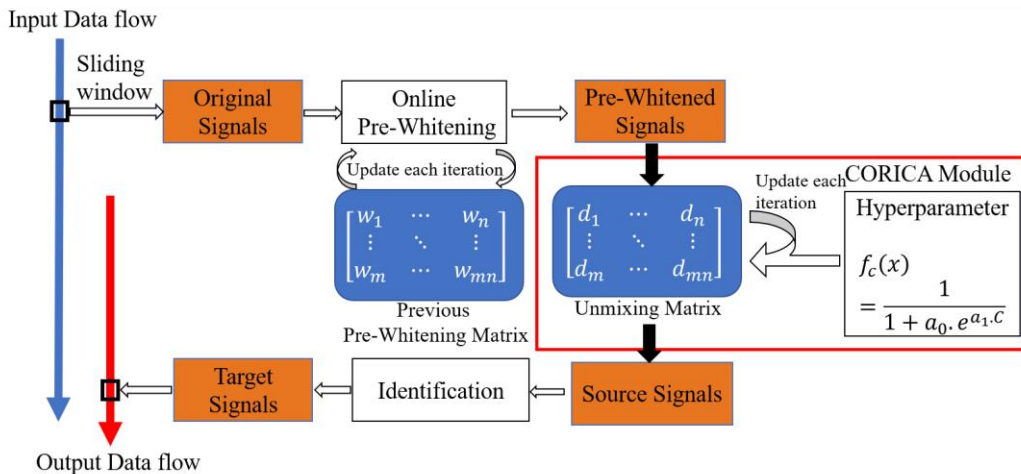


Figure 1. Flowchart of the CORSS framework

$$\Delta W = \eta \left(I + (1-2f)y^{*T} \right) W$$

$$\text{with } f = \frac{1}{1 + a_0 \cdot e^{-a_1 y^*}} \quad (3)$$

where I is the identity matrix, η is the learning rate, y is the component matrix, f is the cost function which is fitted to the CDF of cardiac signal, a_0 and a_1 are constant. By adjusting the cost function, they achieve more accurate result in real time artifact rejection. However, since the basic update rule of the unmixing matrix as shown in formula (3), the author method a faster estimation of the unmixing matrix is desired.

D. ORICA

AKHTAR et al. [16] proposed an BSS algorithm that achieves incremental updates of the unmixing matrix through a recursive procedure. This method achieves results comparable to those offline ICA with faster convergence. They dynamically update the unmixing matrix in real-time and perform online pre-whitening to achieve single-threaded, convenient real-time separation of source signals. According to formula (4):

$$W_{n+1} = W_n + \frac{\lambda_n}{1-\lambda_n} \left[I - \frac{y_n \cdot f^T(y_n)}{1 + \lambda_n (f^T(y_n) \cdot y_n - 1)} \right] W_n \quad (4)$$

where W_n is the unmixing matrix, $y_n = W_n x_n$ is the component matrix, λ_n is a forgetting factor, $f(\cdot)$ is the nonlinear function. With this block-update rule, changes in source patterns and non-stationarity can be addressed, since the ICA model is adaptively updated using the natural gradient of the Infomax ICA rule while the forgetting factor of the algorithm controls the adaptivity to new data and stationarity changes, achieving single-threaded, convenient real-time separation of source signals [23]. However, like most gradient descent algorithms, this approach separates signals at a preliminary level and does not further optimize the algorithm based on the characteristics of the desired signals [17]. It doesn't perform well facing complex real-world condition.

III. METHODS

A. The CORSS framework

The flowchart of the proposed CORSS framework is illustrated in Figure 1. From a segment of electrophysiological signal, initially, the data within a sliding window serves as the raw input and fed into the online pre-whitening module for updating the whitening matrix. Following this, the data is

directed to the constrained online recursive ICA (CORICA) module, where, based on specific cost function from characteristics of the desired signal, the updated demixing matrix obtained from the previous demixing matrix, according to specific update rules, is used to separate sources that better align with the current moment. After that, an identification process is performed based on the features required for the signal, facilitating real-time acquisition of the desired signal sources.

1) . Online Recursive Pre-Whitening

Most BSS methods require pre-whitening the data, which reduces the number of independent parameters and improves convergence. In this study, an online recursive pre-whitening method [10] is employed for real-time data pre-whitening, as shown in formula (5):

$$M_{n+1} = M_n + \frac{\lambda_n}{1-\lambda_n} \left[I - \frac{v_n \cdot v_n^T}{1 + \lambda_n (v_n^T \cdot v_n - 1)} \right] M_n \quad (5)$$

where, n is the number of iterations, M_n is the whitening matrix, $v_n = M_n x_n$ is the pre-whitened data, λ_n is the forgetting factor, I is the identity matrix. Through online recursive pre-whitening, we obtained signals that are more suitable for BSS, which are then fed into the next step, the CORICA module.

II) . Constrained Online recursive ICA

Traditional block-update rules for Infomax-based ICA algorithms are known to be computationally expensive and time-consuming [24], and often lack prior information about target signals. Therefore, in this study, we adopt a multiple measurement vector approach [24] and implement updates on short blocks of samples, with prior information about the target signal which correspond to the natural-gradient version of Infomax [25]:

$$W_{n+L} \approx \left(\prod_{l=n}^{n+L-1} \frac{1}{1-\lambda_l} \right) \cdot \left[I - \sum_{l=n}^{n+L-1} \frac{y_l \cdot f^T(y_l)}{\frac{1-\lambda_l}{\lambda_l} + f^T(y_l) \cdot y_l} \right] W_n \quad (6)$$

$$\text{with } f^T = 1 - \frac{2}{1 + a_0 \cdot e^{-a_1 \cdot y}}$$

where W_n denotes the previous unmixing matrix and W_{n+L} denotes the updated unmixing matrix, L denotes the window length, λ_n is the forgetting factor, $y_l = W_n v_l$ is the component matrix, v_l is the pre-whitened data in the shift window, $f(\cdot)$ is the cost function which is nonlinear. We use this simple update

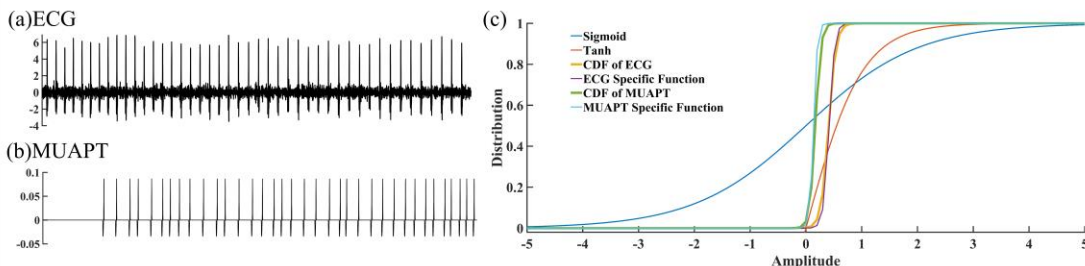


Figure 2. Example of EMG and MUAPT signals, with their CDF. Sigmoid function, tanh function and specific cost function correspond to their CDF are also shown.

rule as well as modify the cost function, that is, to determine a set of specific hyperparameter according to the specific characteristics of the signals, tailoring it to better suit the specific signal sources.

III) . *The choice of the cost function*

By fitting a function that closely resembles the target CDF as the cost function, prior information about the signal can be incorporated into the computation process [20], yielding results that approach the ideal signal more closely. For specific downstream tasks, modifying the cost function to better fit the target signal facilitates algorithm convergence. Electrophysiological signals often exhibit a pulse-like nature, such as common ECG signals and motor unit action potential trains (MUAPT) in EMG decomposition. As illustrated in Figure 2, unlike typical sigmoid or tanh functions for ICA [16], the distribution function of pulsatile electrophysiological signals is approximated based on each pulse cycle by setting a set of hyperparameter.

B. *Experiment and data description*

The proposed approach was tested on the following two distinct real-time biomedical signal processing tasks. We evaluated the online processing effectiveness of the proposed method for these tasks to demonstrate its efficacy in real-time electrophysiological signal processing.

I) . *Real-time sEMG Decomposition*

As sEMG represents the algebraic summation of MUAPT from various active motor units within the electrode's recording range, EMG decomposition is utilized to provide timing information regarding MU discharges. In this experiment, we employed eight sets of 64-channel sEMG data collected using high-density surface electrodes on the APB muscle. The decomposition was also performed using the offline PFP method, which has been previously validated with dual-source verification, to extract MUs as the reference.

The sEMG data are collected and pre-processed by the following step: Eight subjects (age: 26.30 ± 1.89 years) without any known muscular injuries or neuromuscular disorders participated in this study. The experimental protocol was approved by the Ethics Review Committee of University of Science and Technology of China (USTC, Hefei, Anhui, China, under Application No. 2022-N(H)-163). Prior to any experimental procedures, all subjects provided informed and signed consent. SEMG signals were recorded from the abductor pollicis brevis (APB) muscle in the dominant hand of each subject. The recording electrode array was a flexible multi-channel setup arranged in an 8 rows \times 8 columns configuration. Each electrode probe had a diameter of 2mm with an inter-electrode distance of 4mm between consecutive electrodes. This study employed a reliable, homemade, multi-channel sEMG data recording system, as previously validated in our research [26]. Prior to electrode placement, the APB muscle of the test hand was prepared with medical alcohol. Subsequently, the recording electrode array was fully positioned on the APB muscle. In each data recording trial, subjects were instructed to perform an isometric contraction of the thumb, gradually increasing the muscle force from 0 to the max level in 2 seconds and maintaining it for 3 seconds.

Before proceeding with sEMG data processing, several preprocessing steps were undertaken to reduce noise contamination. Initially, we inspected all the channels of the recorded sEMG signals, and a few channels (typically two to five channels) with a low signal-to-noise ratio were discarded. The sEMG signals within the remaining channels were then passed through a 20–500 Hz Butterworth band-pass filter to eliminate potential low-frequency or high-frequency interference. Power line interference was also removed using a 50 Hz second-order notch filter. The final data input format is $64 \times n$, where n represents the number of sample points.

Since the goal of this task is to extract MU source signals, we set a_0 in the cost function to 3 and a_1 to -25, which aligns with the PDF of MU.

II) . *Real-time Non-invasive Respiratory Intent Monitoring based on sEMGdi*

Using sEMGdi for non-invasive respiratory intent monitoring provides direct reflection of neural commands, and is considered state-of-the-art in clinical respiratory monitoring technology [27]. However, surface-collected EMGdi signals typically come with significant ECG artifacts and noise. In this experiment, we apply the proposed method to separate respiratory signals from 8 sets of actual recordings to evaluate the performance of real time sEMGdi extraction.

The sEMGdi data are collected and pre-processed by the following step: eight health subjects (mean age: 26.30 ± 1.89 years) participated in the study. The experimental protocol was approved by the Biomedical Ethics Review Board of USTC (Hefei, Anhui, China, under Application No. 2024KY188). Prior to commencing the experiment, informed consent, duly signed by the subjects was obtained.

Multi-channel sEMGdi signals were recorded from the skin overlying the right costal arch of each participant, specifically between the 8th and 10th rib cartilages [28]. A flexible 32-channel monopolar electrode array, arranged in a 4×8 grid, was utilized for the recordings. Each electrode had a diameter of 2 mm, with an inter-electrode distance of 4 mm. Data acquisition employed a multi-channel surface electromyogram recording system (FlexMatrix Inc., Shanghai, China), featuring a two-stage amplifier with a total gain of 60 dB, band-pass filtered at 1-500 Hz per channel, and an analog-to-digital converter (RHD 2132, Intan Technologies) sampling at 1 kHz.

Following skin preparation using medical alcohol, the electrode array was positioned over the right costal arch. An Ag-AgCl-based self-adhesive surface electrode served as the reference, placed superior to the tip of the xiphoid process, as depicted in Figure 1(b). During each trial, subject was instructed to breathe at various intensities and rates. The duration of sEMGdi signal measurement ranged from 15 seconds to 2 minutes. The recorded raw sEMGdi data were generally pre-processed to reduce the noise contamination. A Butterworth bandpass filter set at 20-150 Hz was applied to eliminate the potential low-frequency motion artifacts and high-frequency environmental interferences. Subsequently, a set of notch filters were utilized to remove power line interference as well as its harmonics. The final data input format is $32 \times n$, where n represents the number of sample points.

Since the goal of this task is to separate EMGdi and ECG source signals, we set a_0 in the cost function to 0.5 and a_1 to -10, which aligns with the PDF of ECG signals therefore can have a better separation.

C. Performance evaluation

For sEMG decomposition task, in order to assess decomposition performance, the decomposition matching rate (MR) is calculated as follows:

$$MR = \frac{2N_{com}}{N_{online} + N_{ref}} \quad (7)$$

where N_{online} is the number of spikes of the online decomposition results, N_{ref} denotes the number of the reference spike acquired by offline PFP, and N_{com} denotes the number of common spikes appearing in both online result and reference. We also calculated the time delay of different window length during processing step, to evaluate real-time usability of the proposed method.

For sEMGdi extraction task, we also use the MR described in Equation 7 to assess respiratory triggering performance. Here, N_{ref} denotes the number of reference breathing triggers, N_{online} denotes the number of correctly identified breathing triggers, when the envelope of the extracted EMGdi signal rises to 30% of its peak value, we consider this as triggering a breath. If the timing of this trigger detected by the online method differs from the reference trigger by within 50ms, it is considered a correctly identified trigger time. The EMGdi extracted using offline methods mentioned in [29] serves as reference to assess the accuracy of real-time respiratory triggering.

Furthermore, since the task of sEMG decomposition does not involve waveform considerations, we conducted more quantitative analyses on the effectiveness of the methods based on recovered signals in the EMGdi extraction task. We employ the Root Mean Square Error (RMSE) and correlation (Corr) between the processed signal envelope and the reference envelope to quantify the extent of signal reconstruction:

$$RMSE = \sqrt{\frac{\sum_{i=1}^n [EMGdi - \widehat{EMGdi}]^2}{n}} \times 100\% \quad (8)$$

where n denotes the number of sample points, $EMGdi$ denotes the reference signal and \widehat{EMGdi} denotes the estimated signal;

$$CORR = \frac{\sum_{i=1}^n (EMGdi - \overline{EMGdi})(\widehat{EMGdi} - \overline{\widehat{EMGdi}})}{\sqrt{\sum_{i=1}^n (EMGdi - \overline{EMGdi})^2 (\widehat{EMGdi} - \overline{\widehat{EMGdi}})^2}} \quad (9)$$

where $EMGdi$ denotes the reference signal, \widehat{EMGdi} denotes the estimated signal and \overline{EMGdi} denotes the average of reference signal.

All the algorithms were implemented on a desktop computer with an Intel Core i5-10400 processor (2.90 GHz) and 16 GB of memory.

In this paper, besides the proposed method, two additional comparison approaches were also employed: Online PFP with a dual-thread update mechanism, and the original ORICA method without incorporating prior information into the function. Note that compared to the proposed method, the processing flow of the original ORICA method is identical except for the replacement of the CORICA module with the ORICA module.

D. Statistical Analysis

In order to examine performance improvement of the proposed method compared with the other comparison method, a series of paired T-tests were applied to the number of MUs and the MR, respectively. The homogeneity of variance test and normality test were conducted before each T-test. The level of significant difference was set as $p < 0.05$. All statistical analyses were performed by SPSS software (ver. 22.0, SPSS Inc. Chicago, IL, USA)

IV. RESULTS

A. The result of online sEMG decomposition

For different window lengths, the execution times of our proposed method and online PFP are presented in Table 1. It

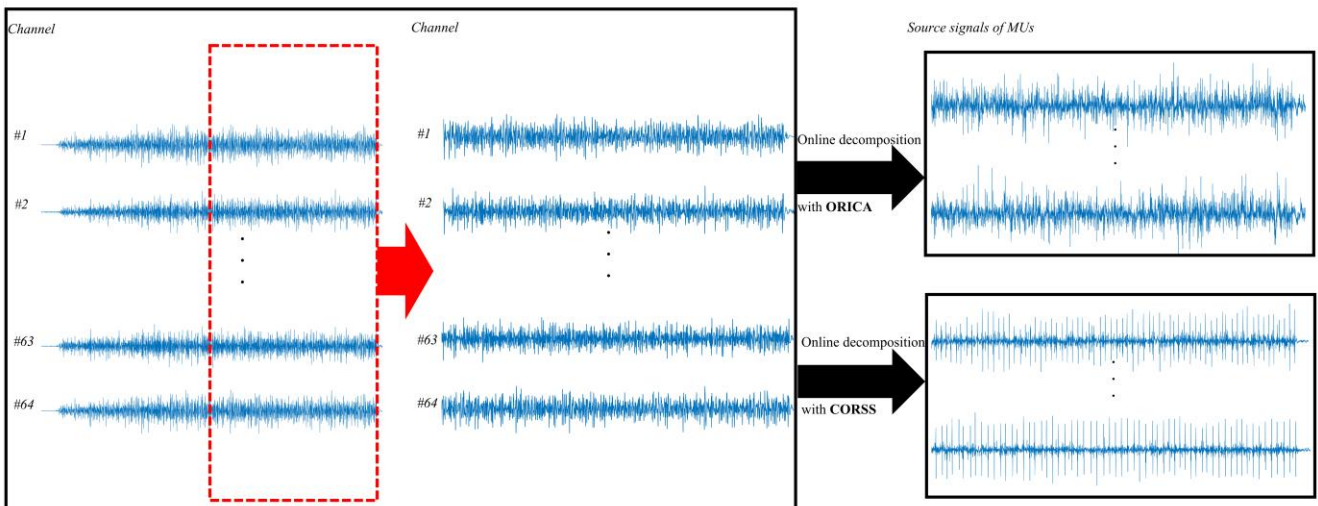


Figure 3. Illustration of sEMG decomposition using different method

Table 2 Average time delay of online PFP and CORSS with different block size on sEMG decomposition task.

Block size	Time delay(s)	
	Online PFP	CORSS
100(0.1s)	0.0125±0.028	0.0053±0.028
200(0.2s)	0.0285±0.073	0.0083±0.028
400(0.4s)	0.0401±0.097	0.0159±0.028
500(0.5s)	0.0394±0.023	0.0181±0.028
1000(1s)	0.0842±0.028	0.0125±0.028
2000(2s)	0.112±0.018	0.0125±0.028

Table 1. Summary of results for sEMG decomposition on eight groups of sEMG data.

Subject	Number of motor units				MR (%)		
	Reference	ORICA	Online PFP	CORSS	ORICA	Online PFP	CORSS
1	8.01±0.94	0.53±0.44	6.72±0.35	6.67±1.26	8.47±3.95	97.48±2.94	94.25±2.48
2	11.75±1.48	0.82±0.76	9.20±0.85	9.21±0.87	10.32±4.21	95.63±1.74	96.76±1.43
3	7.23±0.82	0.64±0.93	6.12±0.56	6.33±0.90	9.95±3.58	97.15±1.96	98.49±1.90
4	8.42±0.91	1.04±0.80	5.32±0.32	5.09±1.26	5.82±8.71	95.91±1.41	96.07±1.66
5	10.73±1.10	1.93±1.39	7.75±1.55	7.97±0.45	13.14±5.18	93.48±2.17	97.34±2.12
6	9.35±1.23	0.73±0.24	5.98±1.02	4.95±0.91	21.66±4.77	91.46±3.90	94.11±3.56
7	12.18±0.72	1.04±0.80	8.19±0.94	9.23±1.14	6.05±3.54	94.29±3.21	94.75±1.85
8	8.50±0.57	0.70±0.33	4.59±1.21	5.42±1.05	19.11±7.35	98.40±1.26	96.25±1.83
Average	9.52±0.95	0.93±0.72	6.73±1.02	6.85±0.87	11.82±3.92	95.48±1.98	96.00±2.04

can be observed that for all block sizes, both CORSS and online PFP exhibit a time delay smaller than the block size itself. This implies that the algorithm's latency is determined by the block size (sampling rate), with computations adding negligible additional influence to the algorithm's operation. However, due to its single-threaded advantage, CORSS achieves faster computation speeds for each block size compared to online PFP.

Figure 3 shows the illustration of MU source signal separation using the proposed CORSS framework and ORICA. It is evident that the quality of source signals derived from CORSS far surpasses those from ORICA. Employing CORSS on 64-channel sEMG data yields clear MU source signals, while using ORICA alone results in poor efficacy which are notably inadequate for sEMG decomposition, failing to further process into MU signals. Table 2 provides quantitative metrics

for the proposed method and comparison approaches in sEMG decomposition. It is evident that ORICA alone cannot effectively separate MU source signals from sEMG data. On average, less than one MU spike train can be identified across various levels of reference, with an average matching rate of only 11.82% among all sequences, indicating ineffectiveness in decomposition. In contrast, the CORSS method and online PFP achieve comparable decomposition results, with matching rates of 96.00% and 95.48% respectively compared to the reference MU spike trains. Figure 4 depicts an example of online decomposition of real sEMG data using the proposed method, showing nearly complete alignment of MU spikes with the reference, albeit with occasional omissions or errors.

B. The result of real-time sEMGdi extraction

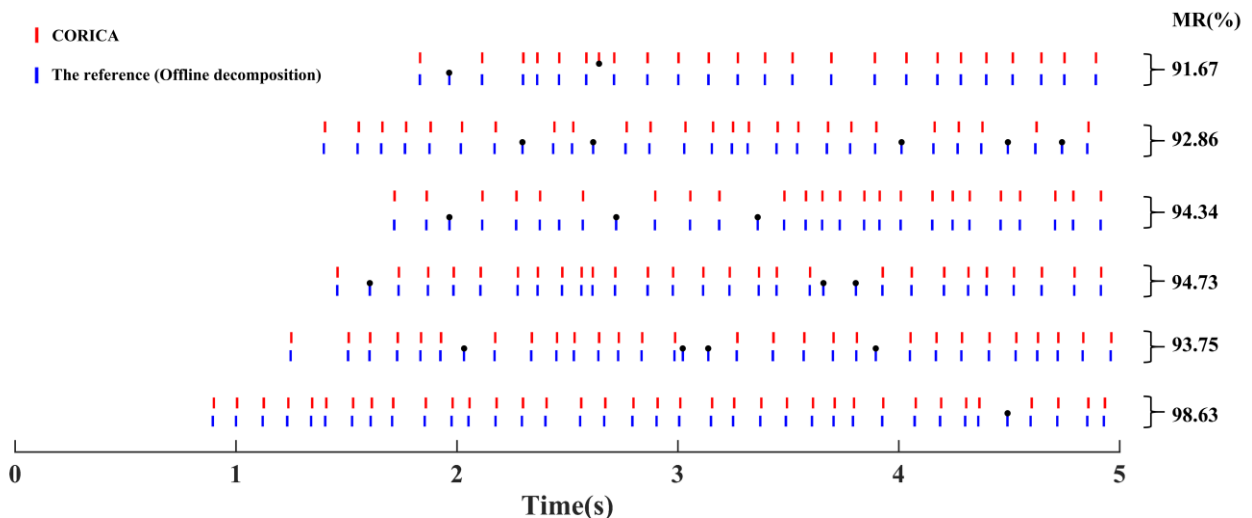


Figure 4. An example of sEMG decomposition using CORSS framework, with the MR of each MU spike train on the right.

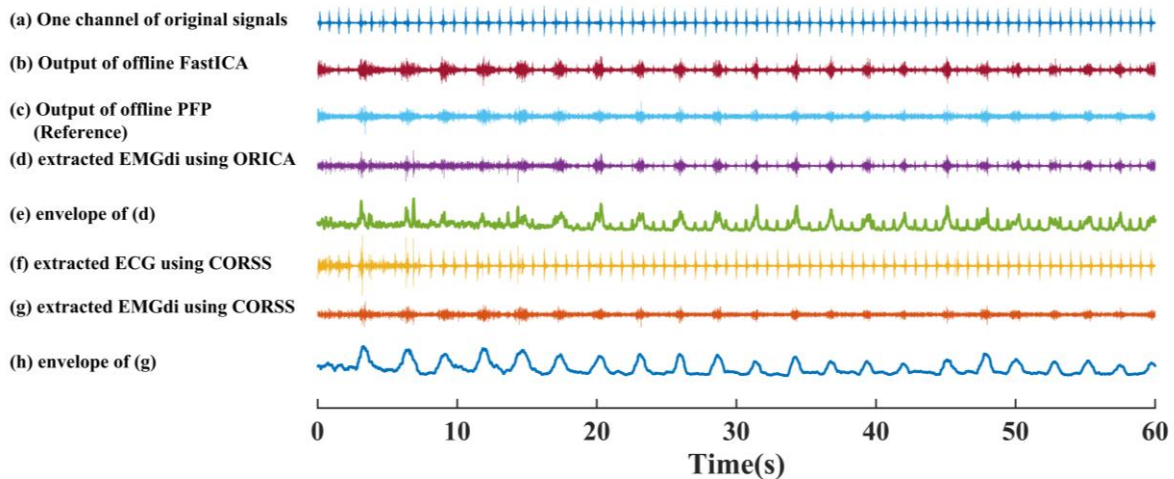


Figure 5. Examples of respiratory-related EMGdi processed by different method. (a) One channel of original signal. (b) Output of offline FastICA. (c) Output of offline PFP, which is used as reference. (d) Extracted EMGdi using ORICA. (e) Envelope of extracted EMGdi using ORICA. (f) Extracted ECG using ORICA. (g) Extracted EMGdi using CORSS. (h) Envelope of extracted EMGdi using CORSS.

Table 3 Quantitative evaluation of EMGdi extraction task with different comparison methods on eight groups of sEMGdi data.

Method	RMSE (%)	MR (%)
ORICA	14.72±4.34	40.47±12.44
Online PFP	8.12±1.21	98.95±1.03
CORSS	6.47±1.80	98.12±1.21

Figure 5 presents a 60-second segment of respiratory signals. It is evident that although the comparative method enhances EMGdi and shows distinct amplitude variations related to respiration, it still exhibits considerable ECG noise, manifested as small spikes in the EMGdi signal which has a significant impact on its envelope, that can easily lead to incorrect judgment of the triggering moment. In contrast, the

proposed method effectively extracts clear EMGdi with an envelope that obviously conforms to the respiratory pattern. The degree of separation between EMG and ECG is greater. This observation is consistently noted across all processed data segments. Table 3 summarizes the quantitative metrics used to describe the performance of EMGdi extraction, where the RMSE values obtained using ORICA are significantly lower compared to those obtained using online PFP and CORSS, as well as the MR in respiratory trigger recognition.

Figure 6 illustrates how Corr and RMSE changes with algorithm runtime. It is observed that within the initial 10-20 seconds after algorithm start, both RMSE and Corr are optimized. Subsequently, they stabilize without significant change. The signal processed by the CORSS framework achieves a Corr of approximately 0.8 by around 7 seconds, reaching approximately 0.98 thereafter. In contrast, ORICA reaches this level only around 20 seconds and stabilizes at approximately 0.87, indicating slower convergence and lower final accuracy compared to CORSS. Similarly, the RMSE obtained by CORSS converges faster than that by ORICA, and the final performance is superior.

V. DISCUSSIONS

Electrophysiological signals collected from the body surface often exhibit overlapping from multiple sources, with the target signal being relatively weak. Current technologies face challenges in real-time separation of these source signals. In this study, we propose a novel real-time processing framework for electrophysiological signals based on BSS. By recursively updating the demixing matrix, we achieve online blind source separation using minimal computational resources. Incorporating prior knowledge through a cost function determined by signal characteristics helps to prevent local convergence and ensures more complete separation. Our

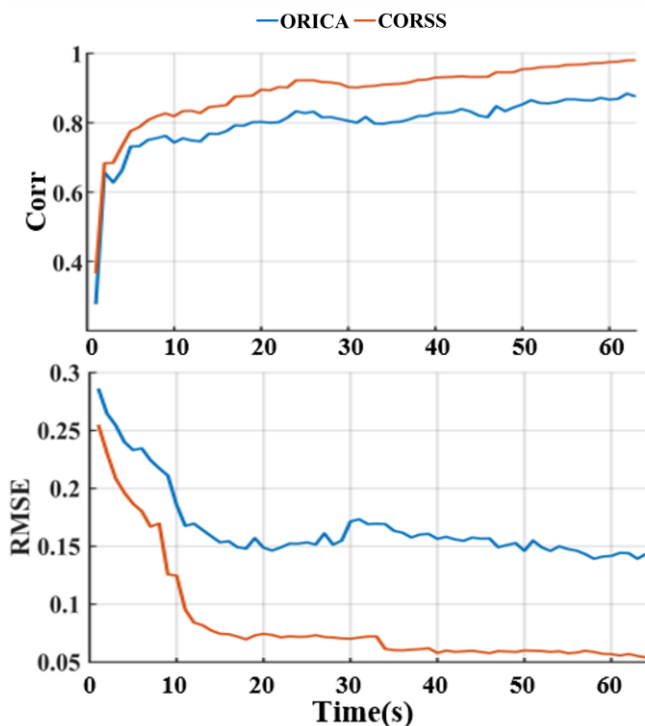


Figure 6. The variations Corr and RMSE over time for respiratory intent monitoring on eight groups of sEMGdi signals, with a window length of 0.1s(100 points). Blue line represents the outcome of ORICA, orange line represents the outcome of CORSS.

method has demonstrated effective performance for both real-time decomposition of surface electromyography and real-time extraction of surface EMGdi signals.

For the task of sEMG decomposition, the algorithm faces stringent demands due to the overlapping nature of actual signals originating from multiple sources. Figure 3 illustrates the preliminary separation results of multi-channel sEMG signals using ORICA and CORSS. CORSS clearly reveals distinct sequences of MU source signals, whereas ORICA, produces noticeably unusable source signals. This is because ORICA lacking prior constraints on pulse-shaped sequences, while CORICA module in CORSS framework combines prior information promote convergence. Figure 4 presents an example of MU spikes derived from source signals obtained via CORSS, demonstrating the efficacy of our method in the real-time electromyographic decomposition domain. Table 2 quantitatively demonstrates that this method achieves performance comparable to that of dual-threaded Online PFP, albeit ORICA, despite its rapid computational speed, yields blurred and still overlapped source signals, resulting in very low MU MR identification. Moreover, as shown in Table 1, although Online PFP performs well in task accuracy, it has higher time delays compared to single-threaded methods. Breuer mentions in [20] that there are three implementations of constrained FastICA: 1) in the initial unmixing matrix, 2) a source specific cost-function, and 3) by measuring the similarity between a reference signal and the extracted sources. Online PFP employs the third approach. Although the offline constrained FastICA module in online PFP used prior information as a constraint to achieve more accurate results, this dual-thread approach determines that the demixing matrix based on the previous moment's signals rather than the current input signal as well as greater computational load, therefore does not have better real-time performance. The proposed method utilizes ORICA's fast computation approach and integrates prior knowledge by modifying the cost function, embedding constraints directly into the computation process, which belongs to the first and second kinds of implementation of constrained FastICA mention earlier, without requiring additional data transmission between threads. Therefore, this approach not only reduces transmission delays but also improves signal updating mechanisms compared to Online PFP. By combining the strengths of ORICA and Online PFP while mitigating their respective weaknesses, the proposed method leverages prior constraints on pulse-shaped electrophysiological signals to facilitate convergence towards ideal signals. Its straightforward, rapid, and constraint-integrated updating rules circumvent the complex computational procedures of dual-threaded methods. Therefore, the proposed method represents a mechanistically superior approach compared to existing methodologies.

For EMGdi extraction task, Figure 5 and Table 3 depict the waveform results and quantitative analyses of different methods in EMGdi extraction. Previous work has demonstrated that using PFP-based methods with constraints effectively extracts surface-acquired EMGdi signals closely correlated with respiratory intent [29], so we establish them as ground truth. Although methods using offline FastICA and ORICA differ in computational processes, their final outcomes

are largely similar due to their lack of relevant information about the target signal, thus less accurate. Incorporating constraints into the algorithms, despite using different constraint methods, notably enhances performance. It is noted that we use the PDF of ECG as the cost function in this task. Since the two main sources in this task are ECG and EMGdi, accurately identifying one source will make the other source clearer.

Figure 6 illustrates RMSE between processed waveforms and references in EMGdi extraction task, showing rapid improvement towards optimal directions until approximately 10 seconds, followed by gradual optimization stabilization, indicating convergence towards optimal solutions in an iterative process, typically within 10-20 seconds. This suggests that the algorithm can effectively operate after about 15 seconds of training on input signals, continuously updating the demixing matrix in real-time. Even with significant signal variations (such as electrode displacement during measurement), the algorithm swiftly resumes normal operation after brief updates. The rapid convergence time is crucial for clinical applications. As mentioned in [30], a common empirical heuristic time for the number of training samples required for separating N stable ICA sources using traditional Infomax-based ICA was kN^2 , where $k > 25$. Therefore, for our 32-channel signal, the heuristic time required for convergence should amount to $32^2 \times 25 = 25600$ samples = 25.6 second with a 1000Hz sample rate. Our experimental results are consistent with this theoretical calculation.

A series of evaluations on these representative tasks demonstrates that the proposed method represents a mechanistically superior approach compared to existing methodologies, which holds significant advantages in real-time processing of electrophysiological signals involving BSS. Its relevance extends to real-time human-machine interaction and clinical monitoring. Given its fast and accurate performance, this method also shows feasibility in other tasks such as clinical fetal electrocardiography (FECG) extraction and real-time motion control.

Currently, a major limitation of this method is its dependence on empirical judgment for adjusting prior parameters. In the future, we can explore methods for automatically adaptation of prior knowledge based on signal characteristics, enabling the framework to intelligently adapt to a broader range of tasks.

VI. CONCLUSION

In this study, we propose a Constrained Online Recursive Source Separation (CORSS) framework for real time electrophysiological signals processing. With a stepwise recursive unmixing matrix learning rule, the algorithm achieves real-time updates with minimal computational overhead. The framework was tested on different downstream tasks with state of the art performance. Our approach demonstrates strong performance across various real-time electrophysiological signals processing tasks, highlighting its significance for applications in real-time human-computer interaction and clinical monitoring.

REFERENCES

- [1] F. Bretschneider and J. De Weille, *Introduction to Electrophysiological Methods and Instrumentation*. 2018, p. 350.
- [2] J. A. Hoffer *et al.*, "Neural signals for command control and feedback in functional neuromuscular stimulation: a review," (in eng), *J Rehabil Res Dev*, vol. 33, no. 2, pp. 145-57, Apr 1996.
- [3] N. Parajuli *et al.*, "Real-time EMG based pattern recognition control for hand prostheses: A review on existing methods, challenges and future implementation," vol. 19, no. 20, p. 4596, 2019.
- [4] K. Wang *et al.*, "High-density surface EMG denoising using independent vector analysis," vol. 28, no. 6, pp. 1271-1281, 2020.
- [5] J. V. J. T. i. c. s. Stone, "Independent component analysis: an introduction," vol. 6, no. 2, pp. 59-64, 2002.
- [6] H. Zhao, X. Zhang, M. Chen, and P. Zhou, "Online Decomposition of Surface Electromyogram Into Individual Motor Unit Activities Using Progressive FastICA Peel-Off," *IEEE Transactions on Biomedical Engineering*, vol. 71, no. 1, pp. 160-170, 2024.
- [7] F. Raimondo, J. E. Kamienskowski, M. Sigman, D. J. C. i. Fernandez Slezak, and neuroscience, "CUDAICA: GPU optimization of infomax - ICA EEG analysis," vol. 2012, no. 1, p. 206972, 2012.
- [8] H. Zhao *et al.*, "Online prediction of sustained muscle force from individual motor unit activities using adaptive surface EMG decomposition," vol. 21, no. 1, p. 47, 2024.
- [9] H. Zhao, X. Zhang, M. Chen, and P. J. I. T. o. B. E. Zhou, "Adaptive Online Decomposition of Surface EMG Using Progressive FastICA Peel-Off," 2023.
- [10] S.-H. Hsu, T. R. Mullen, T.-P. Jung, G. J. I. t. o. n. s. Cauwenberghs, and r. engineering, "Real-time adaptive EEG source separation using online recursive independent component analysis," vol. 24, no. 3, pp. 309-319, 2015.
- [11] A. J. Bell and T. J. J. N. c. Sejnowski, "An information-maximization approach to blind separation and blind deconvolution," vol. 7, no. 6, pp. 1129-1159, 1995.
- [12] A. Hyvärinen and E. J. N. n. Oja, "Independent component analysis: algorithms and applications," vol. 13, no. 4-5, pp. 411-430, 2000.
- [13] J.-F. Cardoso and B. H. J. I. T. o. s. p. Laheld, "Equivariant adaptive source separation," vol. 44, no. 12, pp. 3017-3030, 1996.
- [14] X. Giannakopoulos, J. Karhunen, and E. J. I. j. o. n. s. Oja, "An experimental comparison of neural algorithms for independent component analysis and blind separation," vol. 9, no. 02, pp. 99-114, 1999.
- [15] X.-L. Zhu and X.-D. J. I. S. P. L. Zhang, "Adaptive RLS algorithm for blind source separation using a natural gradient," vol. 9, no. 12, pp. 432-435, 2002.
- [16] M. T. Akhtar, T.-P. Jung, S. Makeig, and G. Cauwenberghs, "Recursive independent component analysis for online blind source separation," in *2012 IEEE International Symposium on Circuits and Systems (ISCAS)*, 2012, pp. 2813-2816: IEEE.
- [17] W. Lu and J. C. Rajapakse, "ICA with Reference," *Neurocomputing*, vol. 69, no. 16, pp. 2244-2257, 2006/10/01/2006.
- [18] L. Wei and J. C. Rajapakse, "Approach and applications of constrained ICA," *IEEE Transactions on Neural Networks*, vol. 16, no. 1, pp. 203-212, 2005.
- [19] J. V. Stone, "Independent component analysis: a tutorial introduction," 2004.
- [20] L. Breuer, J. Dammers, T. P. Roberts, and N. J. J. I. T. o. B. E. Shah, "A constrained ICA approach for real-time cardiac artifact rejection in magnetoencephalography," vol. 61, no. 2, pp. 405-414, 2013.
- [21] X. Tian, X. Zhang, X. Deng, and S. Chen, "Multiway kernel independent component analysis based on feature samples for batch process monitoring," *Neurocomputing*, vol. 72, no. 7, pp. 1584-1596, 2009/03/01/2009.
- [22] M. Chen, P. J. I. T. o. N. S. Zhou, and R. Engineering, "A novel framework based on FastICA for high density surface EMG decomposition," vol. 24, no. 1, pp. 117-127, 2015.
- [23] P. Viana, R. Attux, and S. N. Carvalho, "Comparison Between Online and Offline Independent Component Analysis in the Context of Motor Imagery-Based Brain-Computer Interface," in *IX Latin American Congress on Biomedical Engineering and XXVIII Brazilian Congress on Biomedical Engineering*, Cham, 2024, pp. 302-312: Springer Nature Switzerland.
- [24] J. Chen and X. J. I. T. o. S. p. Huo, "Theoretical results on sparse representations of multiple-measurement vectors," vol. 54, no. 12, pp. 4634-4643, 2006.
- [25] G. D. Brown, S. Yamada, and T. J. J. T. i. n. Sejnowski, "Independent component analysis at the neural cocktail party," vol. 24, no. 1, pp. 54-63, 2001.
- [26] X. Zhang *et al.*, "Muscle force estimation based on neural drive information from individual motor units," vol. 28, no. 12, pp. 3148-3157, 2020.
- [27] L. Piquilloud *et al.*, "Neurally adjusted ventilatory assist improves patient-ventilator interaction," *Intensive Care Medicine*, vol. 37, no. 2, pp. 263-271, 2011/02/01 2011.
- [28] A. Dionne, A. Parkes, B. Engler, B. V. Watson, M. W. J. M. Nicolle, and nerve, "Determination of the best electrode position for recording of the diaphragm compound muscle action potential," vol. 40, no. 1, pp. 37-41, 2009.
- [29] Y. Li, D. Zhao, H. Zhao, X. Zhang, and M. J. a. p. a. Shao, "Extraction of Weak Surface Diaphragmatic Electromyogram Using Modified Progressive FastICA Peel-Off," 2024.
- [30] J. Onton and S. Makeig, "Information-based modeling of event-related brain dynamics," in *Progress in Brain Research*, vol. 159, C. Neuper and W. Klimesch, Eds.: Elsevier, 2006, pp. 99-120.